

# Clusters as ligands, part 3<sup>1</sup>

## Generation of tricobalt cluster carboxylate-bridged iron–cobalt and manganese–cobalt mixed-metal alkoxide cubes from iron and manganese tricobalt cluster metal carboxylates<sup>2</sup>

Xinjian Lei<sup>a</sup>, Maoyu Shang<sup>a</sup>, Thomas P. Fehlner<sup>a,\*</sup>, Rüdiger Werner<sup>b</sup>, Wolfgang Haase<sup>b,3</sup>, Dimitri Hautot<sup>c</sup>, Gary J. Long<sup>c,4</sup>

<sup>a</sup> Department of Chemistry and Biochemistry, University of Notre Dame, Notre Dame, IN 46556, USA

<sup>b</sup> Institut für Physikalische Chemie, Technische Hochschule Darmstadt, Petersenstraße 20, D-64287 Darmstadt, Germany

<sup>c</sup> Department of Chemistry, University of Missouri-Rolla, Rolla, MO 65409-0010, USA

Received 30 September 1996; accepted 15 December 1996

### Abstract

The reaction of the cluster-substituted carboxylic acid,  $(\text{CO})_9\text{Co}_3\text{CCOOH}$ , with  $\text{M}(\text{CH}_3\text{CO}_2)_2$  permits the isolation of  $\text{M}_2\{(\text{CO})_9\text{Co}_3\text{CCO}_2\}_4(\text{THF})_2$ ,  $\text{M} = \text{Mn}$  (**1**),  $\text{Fe}$  (**2**),  $\text{Co}$  (**3**) respectively. Single crystals could not be obtained directly from any of these compounds; however, the slow redox degradation of  $\text{Hg}\{(\text{CO})_9\text{Co}_3\text{CCO}_2\}_2$  in THF leads to crystalline  $[\text{Co}_2\{(\text{CO})_9\text{Co}_3\text{CCO}_2\}_4(\text{THF})_2]$ , which has been characterized by single crystal X-ray structure analysis. Both compounds **1** and **2** react with methanol and the products  $[\text{M}^{\text{II}}\text{Co}_2^{\text{II}}(\text{MeO})_6(\text{MeOH})_2\{(\text{CO})_9\text{Co}_3\text{CCO}_2\}_4] \cdot 2\text{MeOH}$ ,  $\text{M} = \text{Mn}$  (**4**),  $\text{Fe}$  (**5**) respectively, have been isolated as crystalline solids. The formulation of these new mixed-metal cubane clusters is based on analytical data, single crystal X-ray structure analysis, and the Mössbauer spectrum of **5**. The inner  $\text{Co}^{\text{II}}$  centers are derived from sacrificial decomposition of the tricobalt clusters during precipitation of the product. For both **4** and **5** the magnetic susceptibility data show high room temperature magnetic moments which decrease with decreasing temperature consistent with weak antiferromagnetic coupling between the core metal centers and with  $S = 0$  ground states. The formation of these unusual carboxylate coordinated mixed-metal alkoxide cubes derives from the properties of a transition metal cluster as a substituent as well as its tendency to engage in redox chemistry with other metal species. © 1997 Elsevier Science S.A.

**Keywords:** Cobalt cluster; Metal cubane; Carboxylate; Crystal structure

### 1. Introduction

For a long time it has been known that transition metal clusters constitute bulky substituents with unusual electronic properties relative to organic moieties [2–5]. However, the consequences in other areas of chemistry have not been explored. We inadvertently came across an example in the observed stabilization of a tricoordinate boron center by a tetranuclear carbido cluster rela-

tive to base addition [6]. Since then we have explored the consequences of a cluster substituent on the classical coordination chemistry of the carboxylate anion [7]. Thus, we have described cluster metal carboxylates such as  $\text{Zn}_4\text{O}\{(\text{CO})_9\text{Co}_3\text{CCO}_2\}_6$  [1,8] and  $\text{Mo}_2\{(\text{CO})_9\text{Co}_3\text{CCO}_2\}_4$  [9]. The cluster substituent has a distinct effect on synthetic chemistry as well as on compound properties. For example, in terms of chemistry, the enhanced basicity of the cluster carboxylate anion leads to clean displacement of organic carboxylates and, in terms of properties, the low-lying empty metal orbitals of the cluster can lead to large red shifts of metal to ligand charge transfer absorptions.

In some systems the coordination chemistry is perturbed by competitive tricobalt cluster chemistry. It is well known that redox processes are important in facili-

\* Corresponding author.

<sup>1</sup> See Ref. [1] for part 2.

<sup>2</sup> Dedicated to Professor Gottfried Huttner on the occasion of his 60th birthday.

<sup>3</sup> Also corresponding author.

<sup>4</sup> Also corresponding author.

tating various aspects of metal carbonyl cluster chemistry, i.e. substitution [10–13], increases and decreases in cluster nuclearity [14–16] and oxidative coupling [17–19]. This tendency towards redox processes has been used to advantage in synthesis as, for example, in the formation of  $[\text{Fepy}_6][\text{Fe}_4(\text{CO})_{13}]$  from  $\text{Fe}(\text{CO})_5$  and pyridine [20] or in the so-called redox condensation pathway to large metal clusters [21]. Evidence that tricobalt cluster redox chemistry occurs simultaneously with the tricobalt cluster ligand coordination chemistry is provided by the formation of  $\text{Co}_4\text{O}\{(\text{CO})_9\text{Co}_3\text{CCO}_2\}_6$  [1,22] in which the  $\text{Co}^{\text{II}}$  ion originates from the  $(\text{CO})_9\text{Co}_3\text{CCOOH}$  reactant. Although the reaction must be mechanistically complex, the synthesis is a useful one [23]. Herein we describe additional cluster ligand exchange reactions with transition metal acetates and their subsequent redox-induced degradation leading to the formation of new cluster metal carboxylates containing mixed-metal alkoxide cubane-like cores.

## 2. Experimental

### 2.1. Synthetic procedures

All operations were conducted under a nitrogen atmosphere using standard Schlenk techniques. Solvents were distilled before use from drying agents under  $\text{N}_2$  as follows: sodium benzophenone ketyl for hexane, diethyl ether and tetrahydrofuran;  $\text{P}_2\text{O}_5$  for  $\text{CH}_2\text{Cl}_2$ ; manganese metal for  $\text{CH}_3\text{OH}$ .  $\text{Cl}_3\text{CCOOEt}$  was degassed before use. Metal acetates (Aldrich) and  $\text{Co}_2(\text{CO})_8$  (Strem) were used directly as received. Elemental analyses were performed by Galbraith Laboratories, Knoxville, TN and M-H-W Laboratories, Phoenix, AZ.

A new, one-pot synthesis of the cluster ligand,  $(\text{CO})_9\text{Co}_3\text{CCOOH}$ , has been developed. A 500 ml Schlenk flask was charged with 30 g (87.7 mmol) of dicobalt octacarbonyl and 150 ml of distilled THF. The mixture was stirred until the solid dissolved and then 11.0 ml (15.1 g, 85 mmol) of  $\text{CCl}_3\text{COOEt}$  was added slowly by syringe under  $\text{N}_2$  flowing over the solution. The reaction mixture was slowly heated to about 45 °C and CO was produced which was carried away by  $\text{N}_2$ . After 4 h, the reaction mixture was cooled to room temperature and treated with 100 ml of 10% aqueous hydrochloric acid. The aqueous layer was separated and extracted with  $\text{Et}_2\text{O}$ . The resulting organic layer was washed with water and 2 ml of  $\text{CH}_3\text{COOH}$  was added to the solution. The solution was dried over  $\text{MgSO}_4$  for 8 h and then the solution was filtered in air through a 2 cm thick Celite layer. The filtration was kept in a 1000 ml flask and when the solvent was removed under vacuum a large amount of purple crystals formed. To

the purple crystals were added 200 ml of concentrated  $\text{H}_2\text{SO}_4$ . The reaction mixture was stirred for 20 h at room temperature to give a brown solution. The solution was poured into cracked ice and the resulting brown powder was extracted with  $\text{CH}_2\text{Cl}_2$ . The organic layer obtained was washed with water several times until the aqueous layer became colorless and then 5 ml of  $\text{CH}_3\text{COOH}$  was added. The solution was dried over  $\text{MgSO}_4$  for 8 h and then filtered in air through a 2 cm thick Celite layer. The solvent was removed on a rotary evaporator to give 17.0 g (35 mmol) of black crystals. The overall yield is 60% based on total Co.

#### 2.1.1. $[\text{Mn}_2\{(\text{CO})_9\text{Co}_3\text{CCO}_2\}_4(\text{THF})_2]$ (1)

$\text{Mn}(\text{CH}_3\text{CO}_2)_2 \cdot 4\text{H}_2\text{O}$  (0.4 mmol; 0.098 g) and  $(\text{CO})_9\text{Co}_3\text{CCOOH}$  (0.8 mmol; 0.388 g) were loaded into a 100 ml Schlenk flask equipped with a rubber septum and a magnetic stirring bar. This flask had been evacuated and refilled with nitrogen gas several times before 25 ml of  $\text{CH}_2\text{Cl}_2$  was added to the flask via syringe with rapid stirring. The reaction mixture was stirred for 20 h at room temperature to give a precipitate and a purple solution.  $\text{CH}_2\text{Cl}_2$  was removed under vacuum and the residual dark-red solid was washed with hexane. The red-brown solid obtained was then dissolved in 30 ml of THF and stirred for 5 h to give purple solution. THF was slowly removed under vacuum and 0.410 g of dark-red microcrystals was obtained. The corresponding yield based on total Co was 93%. Spectroscopic and analytical data for  $\text{Mn}_2\{(\text{CO})_9\text{Co}_3\text{CCO}_2\}_4(\text{THF})_2$ . Anal.: calc'd for  $\text{C}_{52}\text{H}_{16}\text{Co}_{12}\text{Mn}_2\text{O}_{46}$ : C, 28.47; H, 0.74; Co, 32.24; Mn, 5.01; found: C, 28.35; H, 0.90; Co, 31.78; Mn, 5.03. IR (KBr,  $\text{cm}^{-1}$ ): 2107s, 2051vs,br, 2044vs,sh, 1598w, 1434w, 1374m, 1338w,sh, 761m, 536m, 529m, 500s.

#### 2.1.2. $[\text{Fe}_2\{(\text{CO})_9\text{Co}_3\text{CCO}_2\}_4(\text{THF})_2]$ (2)

$\text{Fe}(\text{CH}_3\text{CO}_2)_2$  (0.4 mmol; 0.070 g) and  $(\text{CO})_9\text{Co}_3\text{CCOOH}$  (0.8 mmol; 0.388 g) were loaded into a 100 ml Schlenk flask equipped with a rubber septum and a magnetic stirring bar. This flask had been evacuated and refilled with nitrogen gas several times before 25 ml of THF was added to the flask via syringe with rapid stirring. The mixture was stirred for 20 h at room temperature to give a purple solution. THF was removed under vacuum and the residual dark-red solid was dissolved in 20 ml of  $\text{CH}_2\text{Cl}_2$  to which 10 ml of hexane was added. The mixture was stirred for 10 h and all solvents were removed under vacuum. The red-brown solid obtained was washed with hexane. The yield is 80% based on total Co. Anal.: calc'd for  $\text{C}_{52}\text{H}_{16}\text{Co}_{12}\text{Fe}_2\text{O}_{46}$ : C, 28.45; H, 0.73; found: C, 28.57; H, 1.02. IR (KBr,  $\text{cm}^{-1}$ ): 2109s, 2055vs, 2049vs,sh, 1581w, 1436w, 1374m, 1341w,sh, 748w, 719m, 551m, 529s, 502s.

2.1.3.  $[\text{Co}_2\{(\text{CO})_9\text{Co}_3\text{CCO}_2\}_4](\text{THF})_2$  (**3**)

(a) Reaction of 254 mg (0.8 mmol)  $\text{Hg}(\text{CH}_3\text{CO}_2)_2$  and 776 mg (1.6 mmol) of  $(\text{CO})_9\text{Co}_3\text{CCOOH}$  in  $\text{CH}_2\text{Cl}_2$  at room temperature gives a dark-red precipitate and a purple solution.  $\text{CH}_2\text{Cl}_2$  was removed under vacuum and the dark-red powder was dissolved in THF and stirred for 5 h to give a purple solution and a gray precipitate. The purple solution was kept undisturbed for several hours and filtered through 1 cm thick Celite. When the solution was kept in a refrigerator without filtering through Celite, tiny droplets of Hg metal or a Hg mirror would appear on the bottom of the flask after several days. The filtrate was layered with  $\text{Et}_2\text{O}$  and kept at room temperature for 3 days to afford 400 mg (53% yield based on Co) of (**3**). Large crystals suitable for X-ray diffraction were grown by layering the filtrate with hexane in a 5 mm glass tube with a narrow neck. IR (KBr,  $\text{cm}^{-1}$ ): 2108m, 2041vs, 2010sh, 1574w, 1545w, 1368m, 1337w, 1068w, 1037w, 884w, 784w, 753m, 713w, 555m, 530m, 515m, 502m, 474w. Anal.: calc'd for  $\text{C}_{52}\text{H}_{16}\text{Co}_{14}\text{O}_{46}$ : C, 28.37; H, 0.73; Co, 37.47; found: C, 28.16; H, 0.56; Co, 36.12.

(b) Solid  $\text{Co}(\text{CH}_3\text{CO}_2)_2 \cdot 4\text{H}_2\text{O}$  (0.2 mmol; 0.049 g) and  $(\text{CO})_9\text{Co}_3\text{CCOOH}$  (0.4 mmol; 0.194 g) was loaded into a 100 ml Schlenk flask equipped with a rubber septum and a magnetic stirring bar. This flask had been evacuated and refilled with dinitrogen several times before 15 ml of THF was added to the flask via syringe. The reaction mixture was stirred for 20 h at room temperature to give a purple solution. THF was removed under vacuum to yield a red-brown solid. The solid was dissolved in 10 ml of THF and the resulting

solution was filtered. The filtrate was layered with hexane and several days later a red-brown precipitate appeared on the bottom of the flask. After washing with hexane, the solid state IR spectrum was that of **3**. In contrast, when the solid was dissolved in  $\text{CH}_2\text{Cl}_2$ , crystals of  $\text{Co}_4^{\text{II}}\text{O}\{(\text{CO})_9\text{Co}_3\text{CCO}_2\}_6$  were isolated as proved by solid state IR and unit cell constants from X-ray diffraction.

2.1.4.  $[\text{Mn}_2\text{Co}_2(\text{MeO})_6(\text{MeOH})_2\{(\text{CO})_9\text{Co}_3\text{CCO}_2\}_4] \cdot 2\text{MeOH}$  (**4**)

$\text{Mn}(\text{CH}_3\text{CO}_2)_2 \cdot 4\text{H}_2\text{O}$  (0.2 mmol; 0.0490 g) and  $(\text{CO})_9\text{Co}_3\text{CCOOH}$  (0.4 mmol; 0.194 g) were loaded into a 100 ml Schlenk flask equipped with a rubber septum and a magnetic stirring bar. This flask had been evacuated and refilled with nitrogen gas several times before 15 ml of THF was added to the flask via syringe with rapid stirring. The mixture was stirred for 20 h at room temperature to give a purple solution. THF was removed under vacuum and 15 ml of MeOH was added to the residual dark-red solid. The mixture was stirred for 5 h to give a red-brown precipitate and a purple solution. Next the MeOH was removed under vacuum and the resulting dark-red solid was dissolved in 10 ml of THF to give a purple solution. The purple solution was layered with 30 ml of MeOH and kept at 4 °C for several days after which 0.080 g of hexagonal-like plate crystals were obtained. The corresponding yield based on total Co was 38%. Spectroscopic and analytical data for  $[\text{Mn}_2\text{Co}_2(\text{CH}_3\text{O})_6(\text{CH}_3\text{OH})_2\{(\text{CO})_9\text{Co}_3\text{CCO}_2\}_4] \cdot 2\text{CH}_3\text{OH}$ . Anal.: calc'd for  $\text{C}_{54}\text{H}_{34}\text{Co}_{14}\text{Mn}_2\text{O}_{54}$ : C, 26.13; H, 1.38; Co, 33.24; Mn, 4.43; found: C, 25.89;

Table 1  
Crystallographic data

	<b>3</b>	<b>4</b>	<b>5</b>
Formula	$\text{C}_{52}\text{H}_{16}\text{Co}_{14}\text{O}_{46}$	$\text{C}_{54}\text{H}_{34}\text{Co}_{14}\text{Mn}_2\text{O}_{54}$	$\text{C}_{54}\text{H}_{34}\text{Co}_{14}\text{Fe}_2\text{O}_{54}$
F.w.	2201.74	2481.78	2483.60
Mo K $\alpha$ radiation $\lambda$ (Å)	0.71073	0.71073	0.71073
Diffractionmeter	Enraf–Nonius CAD4	Enrad–Nonius FAST	Enraf–Nonius CAD4
Temperature (K)	293	180	293
Space group	$I4/m$ (No. 87)	$P\bar{1}$ (No. 2)	$P\bar{1}$ (No. 2)
$a$ (Å)	15.862(4)	14.882(4)	14.982(3)
$b$ (Å)		15.770(3)	15.796(4)
$c$ (Å)	14.624(4)	20.344(4)	20.713(5)
$\alpha$ (deg)		83.66(3)	83.88(3)
$\beta$ (deg)		85.03(3)	85.02(3)
$\gamma$ (deg)		65.49(4)	65.11(3)
$V$ (Å <sup>3</sup> )	3679(2)	4313.3(15)	4416(2)
$Z$	2	2	2
$d_{\text{calc}}$ ( $\text{g cm}^{-3}$ )	1.987	1.911	1.868
$\mu$ (Mo K $\alpha$ ) ( $\text{cm}^{-1}$ )	31.645	29.792	29.634
$R^a$	0.07201	0.0613	0.0437
$R_w^b$	0.09274	0.0696	0.0502

<sup>a</sup>  $R = \sum(|F_o| - |F_c|) / \sum|F_c|$ ; <sup>b</sup>  $R_w = [\sum w(|F_o| - |F_c|)^2 / \sum w|F_o|^2]^{1/2}$  where  $w = 1/[\sigma^2(F_o) + (0.01 F_o)^2 + 2.0]$  (Ref. [24]) for **4** and  $w = 4F_o^2 / \sigma^2(F_o)^2$  for **5**.

Table 2  
Positional and equivalent isotropic thermal parameters for **3**<sup>a</sup>

Atom	x	y	z	B (Å <sup>2</sup> )
Co(1)	0.500	0.500	0.5932(2)	3.36(4)
Co(11)	0.7356(1)	0.7138(1)	0.500	5.50(6)
Co(12)	0.8246(1)	0.6154(1)	0.4161(2)	7.68(5)
O(10)	0.6231(4)	0.5342(5)	0.5767(6)	5.5(2)
C(10)	0.6567(8)	0.5495(9)	0.500	4.6(4)
C(20)	0.7363(9)	0.5938(9)	0.500	4.5(4)
C(11)	0.6622(8)	0.7337(7)	0.594(1)	6.9(4)
O(11)	0.6186(7)	0.7450(7)	0.6489(9)	11.6(3)
C(12)	0.794(1)	0.804(1)	0.500	8.9(7)
O(12)	0.833(1)	0.8683(9)	0.500	15.8(9)
C(21)	0.767(1)	0.618(1)	0.302(1)	15.1(6)
O(21)	0.729(1)	0.620(1)	0.2367(9)	21.7(6)
C(22)	0.915(1)	0.692(1)	0.394(1)	11.0(5)
O(22)	0.9653(7)	0.7370(8)	0.384(1)	16.2(5)
C(23)	0.878(1)	0.517(1)	0.396(2)	18.5(9)
O(23)	0.911(1)	0.455(1)	0.389(1)	26.5(9)
O(31)	0.500	0.500	0.729(1)	6.0(3)
C(31)	0.485(3)	0.572(2)	0.783(3)	13(1) <sup>b</sup>
C(32)	0.461(2)	0.530(2)	0.879(2)	8.9(9) <sup>b</sup>

<sup>a</sup> Anisotropically refined atoms are given in the form of the isotropic equivalent displacement parameter defined as:  $(4/3)[a^2B(1,1) + b^2B(2,2) + c^2B(3,3) + ab(\cos \gamma)B(1,2) + ac(\cos \beta)B(1,3) + bc(\cos \alpha)B(2,3)]$ .

<sup>b</sup> Atoms were refined isotropically.

Table 3  
Selected bond distances (Å) and angles (deg) for **3**

Co(1) Co(1)'	2.727(4)	Co(12) Co(12)'	2.456(3)
Co(1) O(10)	2.041(6)	Co(12) C(20)	1.89(1)
Co(1) O(31)	1.98(2)	Co(12) C(21)	1.90(2)
Co(11) Co(12)	2.437(3)	Co(12) C(22)	1.90(2)
Co(11) Co(12)'	2.437(3)	Co(12) C(23)	1.80(2)
Co(11) C(20)	1.90(1)	O(10) C(10)	1.27(1)
Co(11) C(11)	1.83(1)	C(10) C(20)	1.44(2)
Co(11) C(12)	1.71(2)		
Co(1) Co(1)'	O(10) 83.2(3)	Co(12) Co(12)'	C(23) 99.3(8)
Co(1) Co(1)'	O(31) 180.0(0)	C(20) Co(12)'	C(21) 102.5(6)
O(10) Co(1)'	O(10) 166.44	C(20) Co(12)'	C(22) 141.2(7)
O(10) Co(1)'	O(10) 89.2(3)	C(20) Co(12)'	C(23) 107.3(8)
O(10) Co(1)'	O(31) 96.8(3)	C(21) Co(12)'	C(22) 101.7(8)
Co(12) Co(11)'	Co(12) 60.50(9)	C(21) Co(12)'	C(23) 95.8(9)
Co(12) Co(11)'	C(20) 49.9(3)	C(22) Co(12)'	C(23) 99.8(8)
Co(12) Co(11)'	C(11) 149.1(4)	Co(1) O(10)'	C(10) 124.0(7)
Co(12) Co(11)'	C(12) 102.9(6)	O(10) C(10)'	O(10) 125.0(1)
C(20) Co(11)'	C(11) 100.2(5)	O(10) C(10)'	C(20) 117.5(6)
C(20) Co(11)'	C(12) 146.7(9)	O(10) C(10)'	C(20) 117.5(6)
C(11) Co(11)'	C(12) 101.6(6)	Co(11) C(20)'	Co(12) 79.8(5)
Co(11) Co(12)'	Co(12) 59.75(7)	Co(11) C(20)'	C(10) 119.0(1)
Co(11) Co(12)'	C(20) 50.3(4)	Co(12) C(20)'	C(12) 80.8(6)
Co(11) Co(12)'	C(21) 98.7(5)	Co(12) C(20)'	C(10) 137.2(4)
Co(11) Co(12)'	C(22) 96.4(6)	Co(1) O(31)'	C(31) 124.0(2)
Co(11) Co(12)'	C(23) 155.5(8)	C(31) O(31)'	C(31) 111.0(2)
Co(12) Co(12)'	C(20) 49.6(3)	O(31) C(31)'	C(32) 101.0(3)
Co(12) Co(12)'	C(21) 151.2(6)	C(31) C(32)'	C(32) 113.0(3)
Co(12) Co(12)'	C(22) 99.6(6)	C(31) C(32)'	C(32) 112.0(3)

Numbers in parentheses are estimated standard deviations in the least significant digits.

Table 4  
Positional and equivalent isotropic thermal parameters for **4**<sup>a</sup>

	x	y	z	B (Å <sup>2</sup> )
M(1)	0.28140(8)	0.30127(7)	0.33307(6)	1.21(2) <sup>b</sup>
M(2)	0.10320(8)	0.28452(7)	0.25325(6)	1.21(2) <sup>b</sup>
M(3)	0.15565(8)	0.45398(7)	0.23126(6)	1.26(2) <sup>b</sup>
M(4)	0.31170(8)	0.23950(7)	0.19264(6)	1.45(2) <sup>b</sup>
Co(11)	0.30834(8)	0.65066(7)	0.36533(6)	1.72(2)
Co(12)	0.26974(8)	0.57948(7)	0.47265(6)	1.88(2)
Co(13)	0.13341(8)	0.69541(7)	0.40530(6)	1.91(3)
Co(21)	0.15873(9)	0.05407(7)	0.04445(6)	1.91(3)
Co(22)	0.11205(8)	-0.01655(7)	0.14967(6)	1.62(2)
Co(23)	0.28836(8)	-0.06873(7)	0.11320(6)	1.87(3)
Co(31)	0.64277(9)	-0.02170(8)	0.33421(8)	3.10(3)
Co(32)	0.69639(9)	0.05440(9)	0.23515(8)	2.96(3)
Co(33)	0.67818(9)	0.11697(8)	0.34394(7)	2.87(3)
Co(41)	-0.2400(1)	0.51333(9)	0.14215(7)	2.35(3) <sup>c</sup>
Co(42)	-0.2717(1)	0.57646(9)	0.25180(7)	2.04(3) <sup>c</sup>
Co(43)	-0.22055(9)	0.65814(9)	0.15504(7)	1.94(3) <sup>c</sup>
O(1)	0.2542(4)	0.2056(3)	0.2811(3)	2.3(1)
O(2)	0.1296(4)	0.3732(4)	0.3106(3)	2.4(1)
O(3)	0.3055(4)	0.3560(3)	0.2406(3)	2.6(1)
O(4)	0.1676(4)	0.3398(3)	0.1775(3)	2.3(1)
O(5)	0.2583(4)	0.2453(4)	0.4231(3)	3.4(1)
O(6)	0.0438(4)	0.2319(4)	0.3290(3)	3.2(1)
O(7)	0.1858(4)	0.5257(4)	0.1525(3)	3.1(1)
O(8)	0.3688(4)	0.2730(4)	0.1082(3)	3.7(2)
O(11)	0.2751(4)	0.4190(3)	0.3713(3)	2.2(1)
O(12)	0.1794(4)	0.5327(3)	0.2965(3)	2.3(1)
O(21)	0.1204(4)	0.1783(3)	0.1972(3)	2.0(1)
O(22)	0.2763(4)	0.1413(3)	0.1531(3)	2.4(1)
O(31)	0.4292(4)	0.2089(4)	0.3307(3)	2.7(1)
O(32)	0.4483(4)	0.1621(4)	0.2267(3)	2.7(1)
O(41)	0.0051(4)	0.5166(3)	0.2153(3)	2.4(1)
O(42)	-0.0330(4)	0.3904(3)	0.2286(3)	2.5(1)
O(111)	0.2847(5)	0.6888(5)	0.2218(3)	4.6(2)
O(112)	0.5147(4)	0.5136(6)	0.3597(4)	5.7(2)
O(113)	0.3271(5)	0.8188(4)	0.4040(4)	5.4(2)
O(121)	0.1446(5)	0.4970(5)	0.5501(4)	4.6(2)
O(122)	0.4522(5)	0.4087(5)	0.4888(4)	5.4(2)
O(123)	0.2933(6)	0.7125(5)	0.5540(4)	6.4(2)
O(131)	0.0569(5)	0.7602(5)	0.2731(4)	4.8(2)
O(132)	-0.0277(5)	0.6408(5)	0.4571(4)	4.8(2)
O(133)	0.09236(6)	0.8695(5)	0.4669(5)	6.6(2)
O(211)	0.2851(5)	0.1418(5)	-0.0209(4)	5.1(2)
O(212)	-0.0265(5)	0.2254(5)	0.0358(4)	4.3(2)
O(213)	0.1439(6)	-0.0655(5)	-0.0514(4)	5.9(2)
O(221)	0.1411(5)	-0.0759(4)	0.2907(3)	3.7(2)
O(222)	0.0594(5)	-0.1565(4)	0.0964(4)	4.8(2)
O(223)	-0.0829(5)	0.1344(4)	0.1740(4)	3.9(2)
O(231)	0.4554(5)	-0.0231(5)	0.0587(5)	6.0(2)
O(232)	0.3193(7)	-0.2414(5)	0.0523(4)	6.5(2)
O(233)	0.3687(5)	-0.1338(5)	0.2449(4)	5.0(2)
O(311)	0.4807(6)	0.0032(6)	0.4335(4)	7.0(3)
O(312)	0.5809(6)	-0.1385(5)	0.2594(5)	6.6(2)
O(313)	0.8378(5)	-0.1588(5)	0.3811(4)	5.6(2)
O(321)	0.6669(6)	0.2267(5)	0.1507(4)	5.3(2)
O(322)	0.9122(6)	-0.0607(6)	0.2367(6)	9.1(3)
O(323)	0.6285(8)	-0.0240(6)	0.1366(5)	9.4(3)
O(331)	0.6318(6)	0.3131(5)	0.2977(4)	5.6(2)
O(332)	0.8879(6)	0.0342(6)	0.3797(6)	8.4(3)
O(333)	0.5692(6)	0.1617(6)	0.4705(4)	7.1(2)
O(411)	-0.2077(6)	0.3232(5)	0.1928(5)	7.1(3)
O(412)	-0.1149(7)	0.4570(6)	0.0225(4)	6.4(3)

Table 4 (continued)

	x	y	z	B (Å <sup>2</sup> )
O(413)	-0.4428(7)	0.5944(7)	0.0933(6)	10.3(3)
O(421)	-0.2254(6)	0.4034(5)	0.3379(4)	5.2(2)
O(422)	-0.2430(9)	0.6795(6)	0.3501(4)	8.6(3)
O(423)	-0.4900(6)	0.6644(7)	0.2408(6)	9.6(3)
O(431)	-0.0908(5)	0.6550(6)	0.0385(4)	5.8(2)
O(432)	-0.1452(6)	0.7667(5)	0.2235(5)	7.4(3)
O(433)	-0.4239(6)	0.7881(6)	0.1186(5)	7.0(3)
C(1)	0.2894(7)	0.1081(6)	0.3049(5)	2.6(2)
C(2)	0.0511(6)	0.4205(6)	0.3611(4)	2.1(2)
C(3)	0.3853(6)	0.3870(6)	0.2313(5)	2.5(2)
C(4)	0.1284(6)	0.3584(6)	0.1120(4)	2.1(2)
C(5)	0.2922(8)	0.2547(7)	0.4815(5)	4.1(3)
C(6)	-0.0277(7)	0.1940(7)	0.3218(6)	4.1(3)
C(7)	0.1268(8)	0.6252(6)	0.1357(6)	3.5(3)
C(8)	0.4447(9)	0.2033(8)	0.0704(6)	5.1(3)
C(10)	0.2335(6)	0.5772(5)	0.3867(4)	1.5(2)
C(11)	0.2305(6)	0.5031(5)	0.3490(4)	1.7(2)
C(20)	0.1930(6)	0.0497(5)	0.1323(4)	1.5(2)
C(21)	0.1966(6)	0.1307(5)	0.1633(4)	1.5(2)
C(30)	0.5863(6)	0.1020(6)	0.2939(5)	2.2(2)
C(31)	0.4793(6)	0.1624(5)	0.2835(4)	1.8(2)
C(40)	-0.1563(6)	0.5366(5)	0.1955(4)	1.6(2)
C(41)	-0.0535(6)	0.4767(5)	0.2144(4)	1.8(2)
C(111)	0.2930(6)	0.6748(6)	0.2777(5)	2.5(2)
C(112)	0.4351(7)	0.5674(6)	0.3624(5)	3.0(2)
C(113)	0.3229(7)	0.7526(6)	0.3894(5)	2.9(2)
C(121)	0.1927(7)	0.5308(6)	0.5214(5)	2.5(2)
C(122)	0.3837(6)	0.4745(6)	0.4816(5)	2.6(2)
C(123)	0.2842(8)	0.6612(7)	0.5243(5)	3.6(2)
C(131)	0.0856(7)	0.7368(6)	0.3248(5)	2.9(2)
C(132)	0.0343(7)	0.6634(6)	0.4388(5)	2.6(2)
C(133)	0.1045(7)	0.8047(6)	0.4436(5)	3.3(2)
C(211)	0.2375(7)	0.1073(6)	0.0030(5)	2.5(2)
C(212)	0.0424(7)	0.1592(6)	0.0382(5)	2.7(2)
C(213)	0.1488(7)	-0.0188(6)	-0.0143(5)	3.2(2)
C(221)	0.1316(6)	-0.0553(6)	0.2357(5)	2.1(2)
C(222)	0.0807(6)	-0.1050(6)	0.1174(5)	2.7(2)
C(223)	-0.0075(6)	0.0766(5)	0.1631(5)	2.3(2)
C(231)	0.3903(8)	-0.0420(7)	0.0772(5)	3.4(3)
C(232)	0.3068(8)	-0.1757(6)	0.0748(6)	3.6(3)
C(233)	0.3369(6)	-0.1096(6)	0.1930(5)	2.5(2)
C(311)	0.5493(8)	-0.0084(8)	0.3966(6)	4.2(3)
C(312)	0.6054(8)	-0.0924(7)	0.2873(7)	4.7(3)
C(313)	0.7618(7)	-0.1082(6)	0.3646(6)	3.3(2)
C(321)	0.6806(7)	0.1593(7)	0.1847(5)	3.2(2)
C(322)	0.8299(8)	-0.0162(7)	0.2344(8)	5.1(3)
C(323)	0.6551(8)	0.0073(8)	0.1760(7)	5.3(3)
C(331)	0.6534(7)	0.2367(6)	0.3158(5)	3.0(2)
C(332)	0.8071(7)	0.0669(7)	0.3655(7)	4.8(3)
C(333)	0.6147(8)	0.1409(8)	0.4212(6)	4.9(3)
C(411)	-0.2232(7)	0.4014(7)	0.1732(6)	3.8(3)
C(412)	-0.1633(8)	0.4833(7)	0.0682(5)	3.6(3)
C(413)	-0.3632(8)	0.5618(9)	0.1115(7)	5.7(3)
C(421)	-0.2469(7)	0.4693(6)	0.3028(5)	3.1(2)
C(422)	-0.253(1)	0.6417(7)	0.3100(5)	4.8(3)
C(423)	-0.404(1)	0.628(1)	0.2468(7)	6.7(4)
C(431)	-0.1409(7)	0.6539(7)	0.0824(5)	3.0(2)
C(432)	-0.1760(7)	0.7264(7)	0.1986(6)	3.4(3)
C(433)	-0.3456(8)	0.7404(8)	0.1322(6)	4.3(3)
O(51)	0.1214(5)	0.1767(4)	0.4451(3)	4.3(2)
O(52)	0.3189(5)	0.4486(4)	0.0604(3)	3.9(2)
C(51)	0.159(1)	0.0766(7)	0.4616(7)	5.5(3)

Table 4 (continued)

	x	y	z	B (Å <sup>2</sup> )
C(52)	0.3961(9)	0.4850(9)	0.0546(8)	7.6(4)
Co(41) <sup>y</sup>	-0.2771(6)	0.5218(6)	0.2066(5)	1.8(2) <sup>d</sup>
Co(42) <sup>y</sup>	-0.2459(7)	0.6637(6)	0.2220(5)	2.6(2) <sup>d</sup>
Co(43) <sup>y</sup>	-0.2127(6)	0.5966(6)	0.1141(5)	1.9(2) <sup>d</sup>

<sup>a</sup> Anisotropically refined atoms are given in the form of the isotropic equivalent displacement parameter defined as:  $(4/3)[a^2B(1,1) + b^2B(2,2) + c^2B(3,3) + ab(\cos \gamma)B(1,2) + ac(\cos \beta)B(1,3) + bc(\cos \alpha)B(2,3)]$ .

<sup>b</sup> M = 0.5Mn + 0.5Co.

<sup>c</sup> Occupancy was 0.87.

<sup>d</sup> Occupancy was 0.13.

H, 1.62; Co, 33.40; Mn, 4.44. IR (KBr, cm<sup>-1</sup>): 2108s, 2042vs, 1538m,br, 1368s, 1336m,sh, 1034w, 1020m, 751m, 713m, 552m, 530m, 501s, 474w,sh, 465w,sh.

### 2.1.5. $[Fe_2Co_2(MeO)_6(MeOH)_2\{(CO)_9Co_3CCO_2\}_4] \cdot 2MeOH$ (5)

Fe(CH<sub>3</sub>CO<sub>2</sub>)<sub>2</sub> (0.2 mmol; 0.035 g) and (CO)<sub>9</sub>Co<sub>3</sub>CCOOH (0.4 mmol; 0.194 g) were loaded into a 100 ml Schlenk flask equipped with a capping rubber septum and a magnetic stirring bar. This flask had been evacuated and refilled with nitrogen gas several times before 15 ml of THF was added to the flask via syringe with rapid stirring. The reaction mixture was stirred for 20 h at room temperature to give a purple solution. THF was removed under vacuum and the residual dark-red solid was dissolved in 15 ml of MeOH and stirred for 15 h at 50 °C to give red-brown precipitates and a purple solution. Next the MeOH was removed under vacuum and the resulting dark-red solid was dissolved in 10 ml of THF to give a purple solution. The purple solution was layered with 30 ml of MeOH and kept at 4 °C for several days. Hexagonal plate-like crystals were obtained in 45% yield based on cobalt. Spectroscopic and analytical data for  $[Fe_2Co_2(MeO)_6(MeOH)_2\{(CO)_9Co_3CCO_2\}_4] \cdot 2MeOH$ . Anal.: calc'd for C<sub>54</sub>H<sub>34</sub>Co<sub>14</sub>Fe<sub>2</sub>O<sub>54</sub>: C, 26.12; H, 1.38; Co, 33.22; Fe, 4.50; found: C, 25.83; H, 1.61; Co, 33.30; Fe, 3.94. IR (KBr, cm<sup>-1</sup>): 2109s, 2044vs, 1580w,br, 1369s, 1336m,sh, 1071w, 1020m,br, 750m, 715m, 551m, 530m, 502s, 475w,sh, 462w.

## 2.2. X-ray crystallography

### 2.2.1. $[Co_2\{(CO)_9Co_3CCO_2\}_4(THF)_2]$ (3)

A block-like black crystal with dimensions 0.18 × 0.19 × 0.25 mm<sup>3</sup> was mounted on a glass fiber and data were collected with an Enraf–Nonius CAD4 diffractometer equipped with a graphite crystal monochromated MoK $\alpha$  radiation. The structure was solved by the MULTAN direct methods followed by successive difference Fourier syntheses. Full-matrix least squares re-

Table 5  
Selected atomic distances (Å) and angles (deg) for 4

M(1)	M(2)	3.341(2)	M(4)	O(3)	2.139(6)		
M(1)	M(3)	3.070(1)	M(4)	O(4)	2.095(5)		
M(1)	M(4)	3.056(2)	M(4)	O(8)	1.968(7)		
M(2)	M(3)	3.059(2)	M(4)	O(22)	2.086(6)		
M(2)	M(4)	3.059(2)	M(4)	O(32)	2.025(5)		
M(3)	M(4)	3.347(1)	O(1)	C(1)	1.445(9)		
M(1)	O(1)	2.119(6)	O(2)	C(2)	1.458(9)		
M(1)	O(2)	2.130(5)	O(3)	C(3)	1.45(1)		
M(1)	O(3)	2.048(6)	O(4)	C(4)	1.45(1)		
M(1)	O(5)	2.008(6)	O(5)	C(5)	1.43(1)		
M(1)	O(11)	2.055(6)	O(6)	C(6)	1.44(1)		
M(1)	O(31)	2.074(5)	O(7)	C(7)	1.46(1)		
M(2)	O(1)	2.160(5)	O(8)	C(8)	1.44(1)		
M(2)	O(2)	2.090(7)	O(11)	C(11)	1.264(8)		
M(2)	O(4)	2.048(6)	O(12)	C(11)	1.29(1)		
M(2)	O(6)	1.984(6)	O(21)	C(21)	1.264(8)		
M(2)	O(21)	2.047(6)	O(22)	C(21)	1.26(1)		
M(2)	O(42)	2.081(5)	O(31)	C(31)	1.26(1)		
M(3)	O(2)	2.055(6)	O(32)	C(31)	1.28(1)		
M(3)	O(3)	2.132(5)	O(41)	C(41)	1.27(1)		
M(3)	O(4)	2.146(6)	O(42)	C(41)	1.27(1)		
M(3)	O(7)	1.986(6)	C(10)	C(11)	1.48(1)		
M(3)	O(12)	2.059(6)	C(20)	C(21)	1.51(1)		
M(3)	O(41)	2.078(5)	C(30)	C(31)	1.50(1)		
M(4)	O(1)	2.038(6)	C(40)	C(41)	1.49(1)		
O(1)	M(1)	O(2)	76.2(2)	O(3)	M(1)	O(5)	178.9(3)
O(1)	M(1)	O(3)	84.4(2)	O(3)	M(1)	O(11)	89.0(2)
O(1)	M(1)	O(5)	94.6(3)	O(3)	M(1)	O(31)	88.2(2)
O(1)	M(1)	O(11)	164.9(2)	O(5)	M(1)	O(11)	92.1(2)
O(1)	M(1)	O(31)	87.3(2)	O(5)	M(1)	O(31)	91.3(2)
O(2)	M(1)	O(3)	83.9(2)	O(11)	M(1)	O(31)	106.1(2)
O(2)	M(1)	O(5)	96.3(2)	O(1)	M(2)	O(2)	76.2(2)
O(2)	M(1)	O(11)	89.6(2)				
O(2)	M(1)	O(31)	162.3(2)				
O(1)	M(2)	O(4)	83.1(2)	O(3)	M(4)	O(8)	95.0(3)
O(1)	M(2)	O(6)	95.4(2)	O(3)	M(4)	O(22)	164.2(2)
O(1)	M(2)	O(21)	87.9(2)	O(3)	M(4)	O(32)	89.8(2)
O(1)	M(2)	O(42)	164.8(2)	O(4)	M(4)	O(8)	95.4(2)
O(2)	M(2)	O(4)	84.4(2)	O(4)	M(4)	O(22)	89.5(2)
O(2)	M(2)	O(6)	93.7(3)	O(4)	M(4)	O(32)	165.3(2)
O(2)	M(2)	O(21)	163.6(2)	O(8)	M(4)	O(22)	93.9(3)
O(2)	M(2)	O(42)	90.4(2)	O(8)	M(4)	O(32)	91.1(2)
O(4)	M(2)	O(6)	177.8(3)	O(22)	M(4)	O(32)	103.1(2)
O(4)	M(2)	O(21)	89.8(2)	M(1)	O(1)	M(2)	102.7(2)
O(4)	M(2)	O(42)	88.5(2)	M(1)	O(1)	M(4)	94.6(3)
O(6)	M(2)	O(21)	91.8(2)	M(1)	O(1)	C(1)	120.6(6)
O(6)	M(2)	O(42)	92.6(2)	M(2)	O(1)	M(4)	93.5(2)
O(21)	M(2)	O(42)	104.8(2)	M(2)	O(1)	C(1)	121.2(6)
O(2)	M(3)	O(3)	83.7(2)	M(4)	O(1)	C(1)	118.1(5)
O(2)	M(3)	O(4)	82.9(2)	M(1)	O(2)	M(2)	104.7(2)
O(2)	M(3)	O(7)	176.9(2)	M(1)	O(2)	M(3)	94.3(2)
O(2)	M(3)	O(12)	88.9(2)	M(1)	O(2)	C(2)	120.9(5)
O(2)	M(3)	O(41)	89.6(2)	M(2)	O(2)	M(3)	95.1(2)
O(3)	M(3)	O(4)	75.7(2)	M(2)	O(2)	C(2)	118.6(6)
O(3)	M(3)	O(7)	94.0(2)	M(3)	O(2)	C(2)	117.9(4)
O(3)	M(3)	O(12)	88.6(2)	M(1)	O(3)	M(3)	94.5(2)
O(3)	M(3)	O(41)	163.9(2)	M(1)	O(3)	M(4)	93.7(2)
O(4)	M(3)	O(7)	94.6(2)	M(1)	O(3)	C(3)	117.7(5)
O(4)	M(3)	O(12)	162.9(2)	M(3)	O(3)	M(4)	103.2(3)
O(4)	M(3)	O(41)	89.0(2)	M(3)	O(3)	C(3)	120.6(4)
O(7)	M(3)	O(12)	93.1(3)	M(4)	O(3)	C(3)	121.2(5)
O(7)	M(3)	O(41)	92.1(2)	M(2)	O(4)	M(3)	93.6(2)
O(12)	M(3)	O(41)	105.9(2)	M(2)	O(4)	M(4)	95.2(2)

Table 5 (continued)

O(1)	M(4)	O(3)	84.2(2)	M(2)	O(4)	C(4)	119.1(6)
O(1)	M(4)	O(4)	85.0(2)	M(3)	O(4)	M(4)	104.2(3)
O(1)	M(4)	O(8)	178.9(3)	M(3)	O(4)	C(4)	119.7(4)
O(1)	M(4)	O(22)	87.1(2)	M(4)	O(4)	C(4)	119.6(4)
O(1)	M(4)	O(32)	88.3(2)				
O(3)	M(4)	O(4)	76.6(2)				
M(1)	O(5)	C(5)	123.1(7)	O(11)	C(11)	O(12)	126.5(8)
M(2)	O(6)	C(6)	123.4(6)	O(11)	C(11)	C(10)	118.0(7)
M(3)	O(7)	C(7)	123.3(6)	O(12)	C(11)	C(10)	115.4(6)
M(4)	O(8)	C(8)	121.9(6)	O(21)	C(21)	O(22)	128.2(8)
M(1)	O(11)	C(11)	127.7(6)	O(21)	C(21)	C(20)	116.1(8)
M(3)	O(12)	C(11)	127.8(5)	O(22)	C(21)	C(20)	115.7(6)
M(2)	O(21)	C(21)	127.1(6)	O(31)	C(31)	O(32)	126.6(7)
M(4)	O(22)	C(21)	126.5(5)	O(31)	C(31)	C(30)	117.4(8)
M(1)	O(31)	C(31)	127.9(6)	O(32)	C(31)	C(30)	116.0(7)
M(4)	O(32)	C(31)	127.5(4)	O(41)	C(41)	O(42)	126.4(7)
M(3)	O(41)	C(41)	127.6(4)	O(41)	C(41)	C(40)	117.1(7)
M(2)	O(42)	C(41)	127.7(6)	O(42)	C(41)	C(40)	116.5(9)

refinements were employed. All non-hydrogen atoms were refined with anisotropic thermal parameters in the final cycles, except for the carbon atoms of THF molecules. Additional crystallographic data are given in Table 1 and coordinates and selected bond distances and angles will be found in Tables 2 and 3.

### 2.2.2. $[Mn_2Co_2(MeO)_6(MeOH)_2((CO)_9Co_3CCO_2)_4] \cdot 2MeOH$ (4)

An X-ray quality, hexagonal-like black crystal of (4) was obtained directly by the procedure described above. A crystal of dimensions  $0.30 \times 0.40 \times 0.09$  mm<sup>3</sup> was mounted on a glass fiber with epoxy and data were collected at 180 K with an Enraf–Nonius FAST area-detector diffractometer with an Mo rotating anode source ( $\lambda = 0.71073$  Å) operating at 50 kV and 50 mA. The area detector to crystal distance was 40 mm, and the offset angle of the area detector was 25°. The MADNES package was employed for cell constant determination, image measurement, and intensity data evaluation. The X-ray exposure time for each image was 10 s, and a total of 2230 images were collected. A total of 35 693 measured reflections were considered above background; after averaging, 20 305 unique reflections were available ( $R_{\text{merge}} = 11.0\%$  on intensity). No absorption correction was made and the detailed procedures for small molecules have been described [25]. The structure was solved by the MULTAN direct method in the SDP package followed by successive difference Fourier syntheses. Full-matrix least squares refinements were employed. The core metals were assigned as disordered atoms  $M = 0.5Mn + 0.5Co$  based on the results of chemical analysis because refinements as either four Mn or four Co atoms did not yield reasonable thermal parameters. One of the tricobalt units is also disordered and the site occupancy factors for this tricobalt unit were set to 0.87 and 0.13 respectively. The final thermal

Table 6  
Positional and equivalent isotropic thermal parameters for 5<sup>a</sup>

	x	y	z	B (Å <sup>2</sup> )
M(1)	0.27849(7)	0.30497(6)	0.33090(5)	2.85(2) <sup>b</sup>
M(2)	0.10735(7)	0.28300(6)	0.25578(5)	2.88(2) <sup>b</sup>
M(3)	0.15579(7)	0.45603(6)	0.22768(5)	2.86(2) <sup>b</sup>
M(4)	0.31193(7)	0.24747(7)	0.18946(5)	2.87(2) <sup>b</sup>
Co(11)	0.30063(8)	0.65536(7)	0.35936(6)	4.45(3)
Co(12)	0.26059(8)	0.58717(7)	0.46405(6)	4.72(3)
Co(13)	0.12720(8)	0.70091(7)	0.39696(6)	4.90(3)
Co(21)	0.17233(9)	0.05873(7)	0.04129(6)	4.70(3)
Co(22)	0.11798(7)	-0.00751(7)	0.14225(6)	4.10(3)
Co(23)	0.29471(8)	-0.06198(7)	0.11242(6)	4.40(3)
Co(31)	0.63966(8)	-0.01146(8)	0.32884(7)	5.09(3)
Co(32)	0.69397(8)	0.06932(9)	0.23589(7)	5.26(4)
Co(33)	0.66994(8)	0.12607(8)	0.34526(6)	5.10(3)
Co(41)	-0.2423(1)	0.4998(1)	0.15942(8)	6.44(4) <sup>c</sup>
Co(42)	-0.26244(9)	0.57890(9)	0.25884(7)	4.19(3) <sup>c</sup>
Co(43)	-0.21998(9)	0.6459(1)	0.15521(7)	5.15(4) <sup>c</sup>
O(1)	0.2533(3)	0.2108(3)	0.2794(2)	2.8(1)
O(2)	0.1305(3)	0.3741(3)	0.3099(2)	2.9(1)
O(3)	0.3029(3)	0.3608(3)	0.2365(2)	2.8(1)
O(4)	0.1683(3)	0.3436(3)	0.1773(2)	2.9(1)
O(5)	0.2574(4)	0.2521(3)	0.4201(3)	4.4(1)
O(6)	0.0515(4)	0.2255(3)	0.3280(3)	4.7(1)
O(7)	0.1787(4)	0.5315(3)	0.1506(3)	4.5(1)
O(8)	0.3695(4)	0.2790(4)	0.1052(3)	4.6(1)
O(11)	0.2721(3)	0.4252(3)	0.3651(2)	3.3(1)
O(12)	0.1756(3)	0.5342(3)	0.2924(2)	3.4(1)
O(21)	0.1271(3)	0.1814(3)	0.1961(2)	3.4(1)
O(22)	0.2799(3)	0.1482(3)	0.1530(2)	3.4(1)
O(31)	0.4257(3)	0.2182(3)	0.3267(2)	3.6(1)
O(32)	0.4463(3)	0.1704(3)	0.2259(2)	3.5(1)
O(41)	0.0067(3)	0.5132(3)	0.2163(2)	3.6(1)
O(42)	-0.0256(3)	0.3851(3)	0.2309(3)	3.7(1)
O(111)	0.2802(6)	0.6941(6)	0.2204(4)	10.8(3)
O(112)	0.5035(6)	0.5193(6)	0.3539(6)	13.6(4)
O(113)	0.3219(6)	0.8192(4)	0.3993(4)	10.9(2)
O(121)	0.1428(6)	0.5007(5)	0.5384(4)	9.8(3)
O(122)	0.4428(6)	0.4204(6)	0.4799(5)	11.9(3)
O(123)	0.2778(6)	0.7179(5)	0.5479(4)	12.9(3)
O(131)	0.0474(6)	0.7637(6)	0.2700(4)	10.8(3)
O(132)	-0.0299(5)	0.6471(5)	0.4493(4)	9.8(3)
O(133)	0.0844(6)	0.8781(5)	0.4544(5)	12.8(3)
O(211)	0.2994(5)	0.1442(5)	-0.0223(4)	9.5(3)
O(212)	-0.0098(6)	0.2269(6)	0.0238(4)	11.4(3)
O(213)	0.1612(7)	-0.0626(5)	-0.0517(4)	12.6(3)
O(221)	0.1345(5)	-0.0610(5)	0.2802(4)	8.7(2)
O(222)	0.0733(5)	-0.1505(4)	0.0903(4)	10.8(2)
O(223)	-0.0759(5)	0.1448(5)	0.1564(4)	8.9(2)
O(231)	0.4639(5)	-0.0228(5)	0.0674(4)	10.1(3)
O(232)	0.3304(7)	-0.2334(5)	0.0520(5)	12.9(3)
O(233)	0.3620(5)	-0.1250(5)	0.2427(4)	9.2(3)
O(311)	0.4917(6)	0.0006(6)	0.4327(4)	12.0(3)
O(312)	0.5787(6)	0.1189(5)	0.2499(5)	13.2(3)
O(313)	0.8326(5)	-0.1478(5)	0.3741(4)	9.6(3)
O(321)	0.6631(6)	0.2433(5)	0.1591(4)	9.8(3)
O(322)	0.9073(5)	-0.0435(6)	0.2347(5)	13.4(3)
O(323)	0.6382(7)	-0.0076(6)	0.1341(4)	13.9(3)
O(331)	0.6185(6)	0.3213(5)	0.3090(4)	10.2(3)
O(332)	0.8753(5)	0.0465(5)	0.3818(5)	12.2(3)
O(333)	0.5666(6)	0.1590(7)	0.4709(4)	13.0(3)
O(411)	-0.1978(6)	0.3144(5)	0.2197(5)	11.9(3)
O(412)	-0.1347(8)	0.4376(8)	0.0398(4)	16.0(5)

Table 6 (continued)

	x	y	z	B (Å <sup>2</sup> )
O(413)	-0.4509(7)	0.5633(8)	0.1353(7)	23.7(5)
O(421)	-0.2360(6)	0.4190(5)	0.3491(4)	10.8(3)
O(422)	-0.1960(8)	0.6730(6)	0.3440(4)	15.3(4)
O(423)	-0.4760(6)	0.6874(7)	0.2589(6)	16.1(4)
O(431)	-0.0918(6)	0.6242(8)	0.0404(4)	13.1(4)
O(432)	-0.1539(6)	0.7715(5)	0.2059(5)	13.1(3)
O(433)	-0.4211(5)	0.7665(7)	0.1144(5)	15.2(4)
C(1)	0.2908(6)	0.1116(5)	0.3024(4)	3.8(2)
C(2)	0.0578(5)	0.4207(5)	0.3604(4)	3.7(2)
C(3)	0.3811(5)	0.3943(5)	0.2261(4)	3.9(2)
C(4)	0.1285(5)	0.3607(5)	0.1132(4)	3.8(2)
C(5)	0.3008(8)	0.2538(7)	0.4786(4)	7.2(3)
C(6)	-0.0227(7)	0.1927(7)	0.3260(6)	8.9(4)
C(7)	0.1186(8)	0.6275(6)	0.1321(5)	6.9(3)
C(8)	0.4494(8)	0.2147(8)	0.0679(5)	8.7(4)
C(10)	0.2264(5)	0.5828(5)	0.3799(4)	3.2(2)
C(11)	0.2240(5)	0.5080(5)	0.3434(4)	2.9(2)
C(20)	0.1993(5)	0.0571(5)	0.1290(4)	3.2(2)
C(21)	0.2024(5)	0.1355(5)	0.1625(4)	2.9(2)
C(30)	0.5814(5)	0.1129(5)	0.2926(4)	3.6(2)
C(31)	0.4776(5)	0.1711(4)	0.2804(4)	2.8(2)
C(40)	-0.1537(5)	0.5288(5)	0.2004(4)	3.5(2)
C(41)	-0.0504(5)	0.4710(5)	0.2169(4)	3.3(2)
C(111)	0.2879(7)	0.6804(6)	0.2747(5)	6.1(3)
C(112)	0.4234(8)	0.5733(8)	0.3575(7)	8.8(4)
C(113)	0.3139(7)	0.7556(6)	0.3838(5)	6.7(3)
C(121)	0.1872(8)	0.5368(7)	0.5104(5)	7.1(3)
C(122)	0.3716(7)	0.4-863(8)	0.4750(5)	7.5(3)
C(123)	0.2736(8)	0.6646(7)	0.5162(5)	8.4(3)
C(131)	0.0782(8)	0.7393(7)	0.3198(5)	6.8(3)
C(132)	0.0297(7)	0.6720(6)	0.4304(6)	7.1(3)
C(133)	0.0994(8)	0.8126(7)	0.4322(6)	7.7(3)
C(211)	0.2499(8)	0.1087(7)	0.0020(5)	6.6(3)
C(212)	0.0603(7)	0.1605(7)	0.0297(5)	6.7(3)
C(213)	0.1653(9)	-0.0144(7)	-0.0146(5)	8.6(4)
C(221)	0.1290(7)	-0.0403(7)	0.2237(5)	6.5(3)
C(222)	0.0896(7)	-0.0941(6)	0.1108(5)	6.3(3)
C(223)	0.0001(6)	0.0844(6)	0.1503(5)	5.8(3)
C(231)	0.3973(7)	-0.0404(7)	0.0838(6)	6.7(3)
C(232)	0.3178(8)	-0.1679(7)	0.0771(6)	7.9(3)
C(233)	0.3375(7)	-0.1028(6)	0.1888(5)	6.0(3)
C(311)	0.5537(8)	-0.0069(7)	0.3922(6)	7.9(4)
C(312)	0.6021(7)	-0.0778(7)	0.2818(6)	8.5(3)
C(313)	0.7578(7)	-0.0981(7)	0.3564(6)	6.9(3)
C(321)	0.6788(7)	0.1750(7)	0.1910(5)	7.0(3)
C(322)	0.8255(7)	0.0016(8)	0.2331(6)	8.6(4)
C(323)	0.6609(8)	0.0185(7)	0.1791(6)	8.9(4)
C(331)	0.6425(7)	0.2426(6)	0.3227(6)	7.0(3)
C(332)	0.7945(6)	0.0800(7)	0.3683(6)	7.5(3)
C(333)	0.6061(7)	0.1464(8)	0.4233(5)	8.0(3)
C(411)	-0.2196(8)	0.3954(8)	0.1915(6)	9.9(4)
C(412)	-0.183(1)	0.461(1)	0.0873(6)	11.9(5)
C(413)	-0.3657(9)	0.539(1)	0.1424(9)	16.2(6)
C(421)	-0.2486(8)	0.4835(7)	0.3132(6)	7.3(3)
C(422)	-0.2257(9)	0.6400(7)	0.3092(6)	9.0(4)
C(423)	-0.3903(8)	0.6457(9)	0.2613(7)	10.1(5)
C(431)	-0.1464(9)	0.630(1)	0.0855(6)	10.9(5)
C(432)	-0.1808(8)	0.7245(7)	0.1863(6)	8.0(4)
C(433)	-0.3423(8)	0.7218(9)	0.1297(7)	10.8(5)
O(51)	0.1280(5)	0.1781(5)	0.4408(3)	7.7(2)
O(52)	0.3126(5)	0.4522(5)	0.0606(3)	7.2(2)
C(51)	0.164(1)	0.0794(8)	0.4620(7)	11.0(5)

Table 6 (continued)

	<i>x</i>	<i>y</i>	<i>z</i>	<i>B</i> (Å <sup>2</sup> )
C(52)	0.385(1)	0.492(1)	0.0458(7)	12.7(5)
Co(41) <sup>f</sup>	−0.2087(8)	0.5795(9)	0.1199(7)	6.6(4) <sup>d</sup>
Co(42) <sup>f</sup>	−0.2673(8)	−0.514(1)	0.2124(7)	7.1(4) <sup>d</sup>
Co(43) <sup>f</sup>	−0.240(1)	0.653(1)	0.2135(8)	9.7(6) <sup>d</sup>

<sup>a</sup> Anisotropically refined atoms are given in the form of the isotropic equivalent displacement parameter defined as:  $(4/3)[a^2B(1,1) + b^2B(2,2) + c^2B(3,3) + ab(\cos \gamma)B(1,2) + ac(\cos \beta)B(1,3) + bc(\cos \alpha)B(2,3)]$ .

<sup>b</sup>  $M = 0.5\text{Fe} + 0.5\text{Co}$ .

<sup>c</sup> Occupancy was 0.89.

<sup>d</sup> Occupancy was 0.11.

parameters for these disordered atoms were reasonable. All non-hydrogen atoms were refined with anisotropic thermal parameters in the final cycles. Additional crystallographic data are given in Table 1 and coordinates and selected bond distances and angles will be found in Tables 4 and 5.

### 2.2.3. $[\text{Fe}_2\text{Co}_2(\text{MeO})_6(\text{MeOH})_2\{(\text{CO})_9\text{Co}_3\text{CCO}_2\}_4] \cdot 2\text{MeOH}$ (**5**)

Crystals suitable for X-ray diffraction were grown by layering MeOH on top of a saturated  $\text{CH}_2\text{Cl}_2$  solution of the compound in a 5 mm glass tube with a narrow neck. A block-like black crystal with dimensions  $0.30 \times 0.25 \times 0.19 \text{ mm}^3$  was mounted in a quartz capillary with a small amount of mixed  $\text{CH}_2\text{Cl}_2$ –MeOH solvent and data were collected at room temperature with an Enraf–Nonius CAD4 diffractometer equipped with a graphite crystal monochromator and  $\text{Mo K}\alpha$  radiation. The structure was solved by the MULTAN direct method followed by successive difference Fourier syntheses. Full-matrix least squares refinements were employed. The core metal was assigned as disordered atoms,  $M = 0.5\text{Fe} + 0.5\text{Co}$ , based on the analytical results because refinements with either four Fe or four Co atoms did not afford reasonable thermal parameters. One of the tricobalt units was found to be disordered and the site occupancy factors for this tricobalt unit were set to 0.89 and 0.11 respectively. The final thermal parameters for these disordered atoms were reasonable. All non-hydrogen atoms were refined with anisotropic thermal parameters in the final cycles. Additional crystallographic data are given in Table 1 and coordinates and selected bond distances and angles will be found in Tables 6 and 7.

### 2.3. Physical measurements

FT-IR spectra were measured on a Nicolet 205 spectrometer. Mössbauer spectra of polycrystalline samples of **5** were obtained on a conventional constant acceleration spectrometer which utilized a room temperature rhodium matrix cobalt-57 source and was calibrated at room temperature with natural abundance  $\alpha$ -iron foil.

Table 7

Selected atomic distances (Å) and angles (deg) for **5**

M(1) M(2)	3.267(2)	M(3) O(3)	2.090(4)
M(1) M(3)	3.090(1)	M(3) O(4)	2.086(5)
M(1) M(4)	3.096(1)	M(3) O(7)	1.981(5)
M(2) M(3)	3.097(2)	M(3) O(12)	2.033(5)
M(2) M(4)	3.095(1)	M(3) O(41)	2.050(4)
M(3) M(4)	3.271(1)	M(4) O(1)	2.119(5)
M(1) O(1)	2.089(5)	M(4) O(3)	2.077(5)
M(1) O(2)	2.079(4)	M(4) O(4)	2.063(4)
M(1) O(3)	2.125(4)	M(4) O(8)	1.987(5)
M(1) O(5)	2.000(5)	M(4) O(22)	2.050(6)
M(1) O(11)	2.057(5)	M(4) O(32)	2.028(4)
M(1) O(31)	2.049(4)	O(11) C(11)	1.254(7)
M(2) O(1)	2.070(4)	O(12) C(11)	1.268(8)
M(2) O(2)	2.068(5)	O(21) C(21)	1.252(7)
M(2) O(4)	2.131(5)	O(22) C(21)	1.258(9)
M(2) O(6)	1.974(6)	O(31) C(31)	1.271(8)
M(2) O(21)	2.036(5)	O(32) C(31)	1.262(9)
M(2) O(42)	2.032(4)	O(41) C(41)	1.28(1)
M(3) O(2)	2.132(5)	O(42) C(41)	1.256(8)
O(1) M(1)	O(2) 75.9(2)	O(11) M(1)	O(31) 104.3(2)
O(1) M(1)	O(3) 83.4(2)	O(1) M(2)	O(2) 76.6(2)
O(1) M(1)	O(5) 97.0(2)	O(1) M(2)	O(4) 83.0(2)
O(1) M(1)	O(11) 163.5(2)	O(1) M(2)	O(6) 96.7(2)
O(1) M(1)	O(31) 88.6(2)	O(1) M(2)	O(21) 88.7(2)
O(2) M(1)	O(3) 84.2(2)	O(1) M(2)	O(42) 163.7(2)
O(2) M(1)	O(5) 96.5(2)	O(2) M(2)	O(4) 83.8(2)
O(2) M(1)	O(11) 89.7(2)	O(2) M(2)	O(6) 96.7(2)
O(2) M(1)	O(31) 162.7(2)	O(2) M(2)	O(21) 163.3(2)
O(3) M(1)	O(5) 179.2(2)	O(2) M(2)	O(42) 90.2(2)
O(3) M(1)	O(11) 87.2(2)	O(4) M(2)	O(6) 179.4(2)
O(3) M(1)	O(31) 86.4(2)	O(4) M(2)	O(21) 86.6(2)
O(5) M(1)	O(11) 92.6(2)	O(4) M(2)	O(42) 86.2(2)
O(5) M(1)	O(31) 92.9(2)	O(6) M(2)	O(21) 92.8(2)
O(6) M(2)	O(42) 94.1(2)	O(4) M(4)	O(32) 163.4(2)
O(21) M(2)	O(42) 102.8(2)	O(8) M(4)	O(22) 93.9(2)
O(2) M(3)	O(3) 83.7(2)	O(8) M(4)	O(32) 92.7(2)
O(2) M(3)	O(4) 83.3(2)	O(22) M(4)	O(32) 102.6(2)
O(2) M(3)	O(7) 179.4(2)	M(1) O(1)	M(2) 103.5(2)
O(2) M(3)	O(12) 86.7(2)	M(1) O(1)	M(4) 94.8(2)
O(2) M(3)	O(41) 87.1(2)	M(2) O(1)	M(4) 95.3(2)
O(3) M(3)	O(4) 75.8(2)	M(1) O(2)	M(2) 104.0(2)
O(3) M(3)	O(7) 96.4(2)	M(1) O(2)	M(3) 94.4(2)
O(3) M(3)	O(12) 89.1(2)	M(2) O(2)	M(3) 95.0(2)
O(3) M(3)	O(41) 162.8(2)	M(1) O(3)	M(3) 94.3(2)
O(4) M(3)	O(7) 96.1(2)	M(1) O(3)	M(4) 94.9(2)
O(4) M(3)	O(12) 162.7(2)	M(3) O(3)	M(4) 103.4(2)
O(4) M(3)	O(41) 88.6(2)	M(2) O(4)	M(3) 94.5(2)
O(7) M(3)	O(12) 93.9(2)	M(2) O(4)	M(4) 95.1(2)
O(7) M(3)	O(41) 92.6(2)	M(3) O(4)	M(4) 104.0(2)
O(12) M(3)	O(41) 104.9(2)	M(1) O(11)	C(11) 127.6(5)
O(1) M(4)	O(3) 83.8(2)	M(3) O(12)	C(11) 129.5(4)
O(1) M(4)	O(4) 83.5(2)	M(2) O(21)	C(21) 128.5(5)
O(1) M(4)	O(8) 178.7(2)	M(4) O(22)	C(21) 128.0(4)
O(1) M(4)	O(22) 85.6(2)	M(1) O(31)	C(31) 129.0(4)
O(1) M(4)	O(32) 86.3(2)	M(4) O(32)	C(31) 129.8(4)
O(3) M(4)	O(4) 76.6(2)	M(3) O(41)	C(41) 128.4(4)
O(3) M(4)	O(8) 96.9(2)	M(2) O(42)	C(41) 129.6(5)
O(3) M(4)	O(22) 163.6(2)	O(11) C(11)	O(12) 126.3(7)
O(3) M(4)	O(32) 89.3(2)	O(21) C(21)	O(22) 127.1(7)
O(4) M(4)	O(8) 97.7(2)	O(31) C(31)	O(32) 125.1(5)
O(4) M(4)	O(22) 89.7(2)	O(41) C(41)	O(42) 125.5(6)

The spectra were fit to Lorentzian line shapes by using standard least squares computer minimization techniques.

Solid state magnetic measurements on powdered samples of **4** and **5** were recorded on a Faraday-type magnetometer using a Calm RG electrobalance in the temperature range 4.3–300.4 K. The applied magnetic field was ca. 1.4 T. Details of the apparatus have been described elsewhere [26]. Experimental susceptibility data were corrected for the underlying diamagnetism using Pascal's incremental system. Corrections for diamagnetism were estimated as  $-894 \times 10^{-6} \text{ cm}^3 \text{ mol}^{-1}$  for **4** and  $-890 \times 10^{-6} \text{ cm}^3 \text{ mol}^{-1}$  for **5**.

### 3. Results and discussion

#### 3.1. Neutral quadruply-bridged $M^{II}$ dimers

The reaction of  $M^{II}$  acetates,  $M = \text{Mn, Fe, Co}$  with  $(\text{CO})_9\text{Co}_3\text{CCOOH}$  led to the formation of  $[M^{II}\{(\text{CO})_9\text{Co}_3\text{CCO}_2\}_2]$ , (**1,2,3**). We have previously reported crystallographically characterized examples of this type of cluster metal carboxylate structure for  $\text{Mo}^{II}$  [9] and  $\text{Cu}^{II}$  [27] and, based on the carboxylate bands in the infrared spectra, we formulate the compounds as bridged dimers. However, in no case were crystals of sufficient quality for a single crystal X-ray structure

determination obtained by recrystallization. For example, all attempts to recrystallize the nearly insoluble Co derivative in various solvents led to either precipitation or the isolation of  $\text{Co}_4^{II}\text{O}\{(\text{CO})_9\text{Co}_3\text{CCO}_2\}_6$ . Fortunately, as described below, the cobalt derivative was isolated and crystallized via an alternative route and, based on inter-comparison of IR spectra, it serves as structure proof for all three compounds.

In examining the reactivity of other metal acetates, the reaction of  $\text{Hg}(\text{CH}_3\text{CO}_2)_2$  with  $(\text{CO})_9\text{Co}_3\text{CCOOH}$  was also carried out. Surprisingly, the reaction leads to the isolation of crystalline  $\text{Co}_2\{(\text{CO})_9\text{Co}_3\text{CCO}_2\}_4(\text{THF})_2$  (**3**) in good yield. The spectroscopic properties of this compound are the same as those of the product of cluster ligand, metal acetate exchange reaction. The solid state structure of **3** (Fig. 1) is similar to that of  $\text{Mo}_2^{II}\{\mu\text{-}[(\text{CO})_9\text{Co}_3\text{CCO}_2]\}_4\{(\text{CO})_9\text{Co}_3\text{CCOOH}\}_2$  [9] except for the replacement of the axial  $(\text{CO})_9\text{Co}_3\text{CCOOH}$  ligands with THF. As expected, the dimetal carboxylate core of **3** is also very similar to that of the known  $\text{Co}^{II}$  dimers with organic carboxylate bridges [28–30]. Infrared spectroscopy suggests that the initial product of the exchange reaction with  $\text{Hg}(\text{CH}_3\text{CO}_2)_2$ , which is insoluble in  $\text{CH}_2\text{Cl}_2$ , is  $\text{Hg}\{(\text{CO})_9\text{Co}_3\text{CCO}_2\}_2$ . The product is soluble in THF and in solution a slow redox reaction takes place producing Hg metal and a precipitate of X-ray quality crystals of **3**.

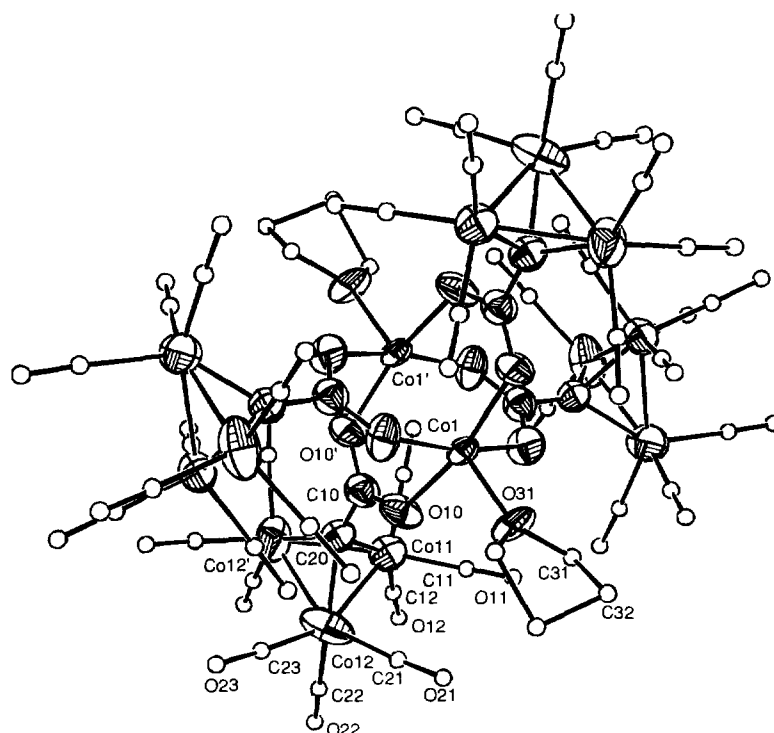


Fig. 1. ORTEP diagram of  $[\text{Co}_2\{(\text{CO})_9\text{Co}_3(\text{CCO}_2)_4\}_2(\text{THF})_2]$  (**3**) with thermal ellipsoids at 40% probability. Note that radii of the carbon and oxygen atoms of the CO ligands and the carbon atoms of the THF molecules are set at arbitrary values for clarity.

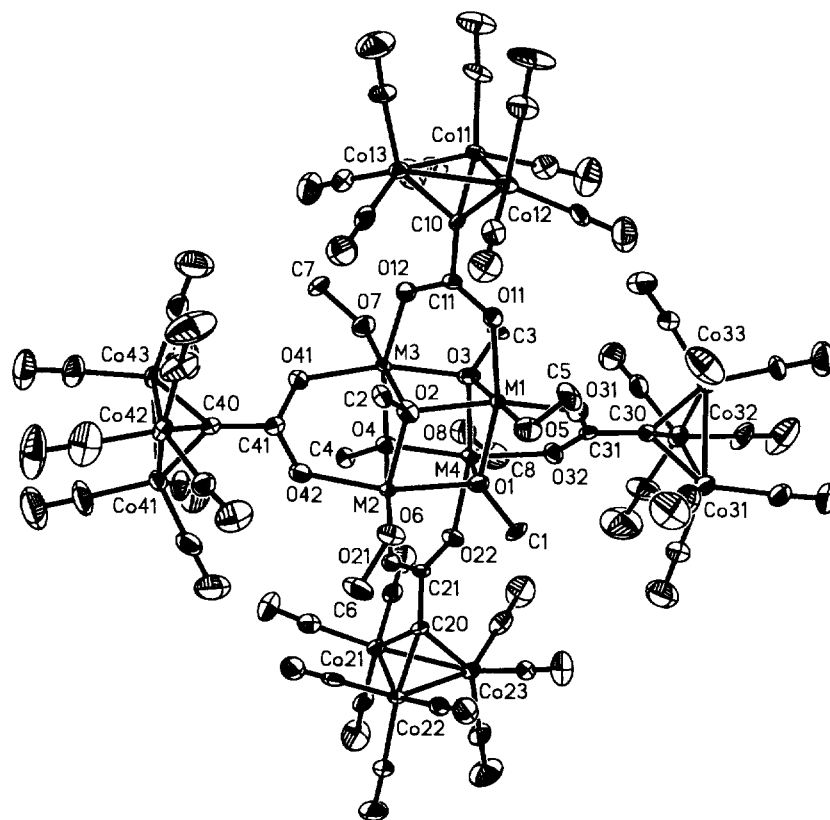


Fig. 2. The ORTEP diagram of  $[\text{Mn}_2\text{Co}_2(\text{MeO})_6(\text{MeOH})_2\{(\text{CO})_9\text{Co}_3\text{CCO}_2\}_4] \cdot 2\text{MeOH}$  (4) with 40% thermal ellipsoids

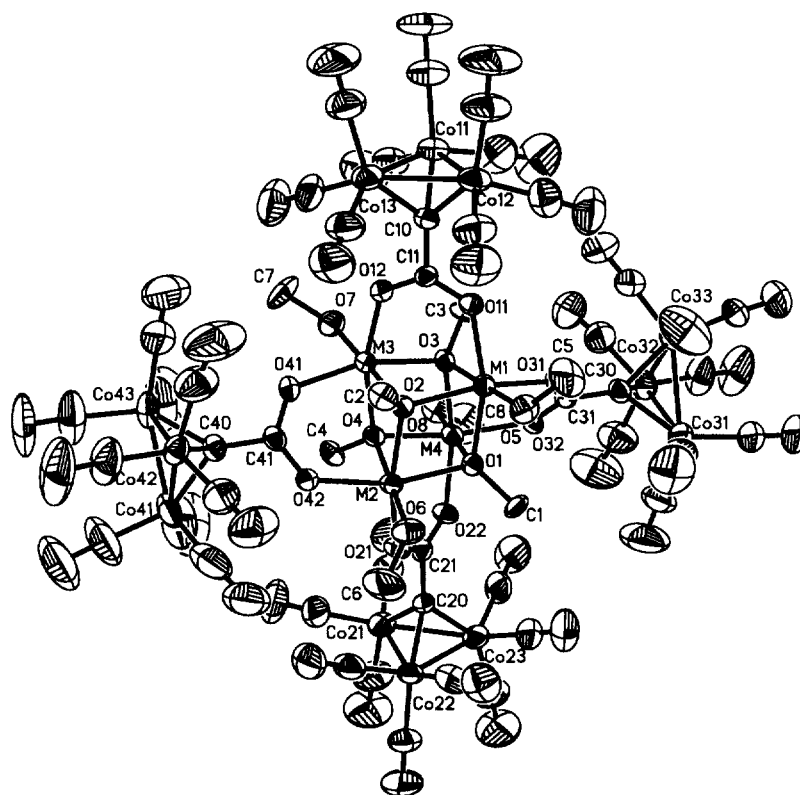


Fig. 3. The ORTEP diagram of  $[\text{Fe}_2\text{Co}_2(\text{MeO})_6(\text{MeOH})_2\{(\text{CO})_9\text{Co}_3\text{CCO}_2\}_4] \cdot 2\text{MeOH}$  (5) with 40% thermal ellipsoids.

Table 8  
Mössbauer spectral hyperfine parameters for **5**

Model	<i>T</i> (K)	$\delta^a$ (mm s <sup>-1</sup> )	$\Delta E_Q$ (mm s <sup>-1</sup> )	$\Gamma$ (mm s <sup>-1</sup> )	Area (%)
Distribution fit	295	0.37 <sup>b</sup>	0.90 <sup>b</sup>	0.24	100
	78	0.49 <sup>b</sup>	0.93 <sup>b</sup>	0.24	100
Doublet fit	295	0.36	1.16	0.43	38
		0.36	0.70	0.43	62
	78	0.49	1.19	0.40	41
		0.49	0.69	0.40	59

<sup>a</sup> Relative to room temperature  $\alpha$ -iron foil.

<sup>b</sup> Distribution weighted average value for the fixed linewidth.

### 3.2. Neutral bridged $M_2Co_2$ cubes

Attempts to recrystallize  $[M^II\{(CO)_9Co_3CCO_2\}_2]$ ,  $M = Mn, Fe$ , by layering a THF solution of  $[M^II\{(CO)_9Co_3CCO_2\}_2]$  with MeOH gave rise to crystalline  $[M_2^{III}Co_2^{II}(MeO)_6(MeOH)_2\{(CO)_9Co_3CCO_2\}_4]$  cubes. Moderate yields of the cubes were obtained by further optimizing the reaction procedure with the incorporation of MeOH as a reagent as described in Section 2. These compounds were characterized as follows.

The molecular structures of  $[M_2^{III}Co_2^{II}(MeO)_6(MeOH)_2\{(CO)_9Co_3CCO_2\}_4]$ ,  $M = Mn, Fe$ , are shown in Figs. 2 and 3. Consideration of the arrangement of the bridging carboxylates over the tetrahedral  $M_2Co_2$  metal core shows that two isomers are possible, one of which is chiral. Unfortunately, the four metal atoms are disordered over the four sites, thereby preventing the detection of any isomerism in the X-ray diffraction experiment. Further, the diffraction experiment did not permit us to locate the hydrogen atoms on the MeOH and/or MeO ligand fragments. Pertinent distances and angles are given in Tables 5 and 7 and a comparison with the values of  $[Fe^III Fe_3^II(OMe)_5(MeOH)_3(OBz)_4]$  [31] as well as closely related compounds [32] show that directly related parameters are similar. Some of the asymmetries found in the  $[Fe^III Fe_3^II(OMe)_5(MeOH)_3(OBz)_4]$  cube core dimensions are also found in the structures of **4** and **5** but the disorder problem in the present structures does not justify discussion.

The different metal occupancies on the four metal sites in the cube core could not be refined and, hence, the crystallographic information does not determine the metal composition. However, the composition is established as follows. Reproducible metal analyses demonstrate that a given cube core contains 50%  $M$  and 50%  $Co$ . Considering the method of synthesis a statistical distribution of  $M_nCo_{4-n}$  species is possible, but this would require a fortuitous 1:1  $M:Co$  ratio in the product. The  $M_2^{III}Co_2^{II}$  formulation of the core, which is unambiguous in the case of  $M = Fe$ , also mitigates against a random distribution of mixed metal species.

The structural parameters associated with the terminal MeOH or MeO<sup>-</sup> ligands bonding to the metal centers reflect metal oxidation states. Although the M–O–C angle is uninformative, the M–O distance is sensitive to the presence of a proton on the oxygen atom. The Fe<sup>III</sup>–OMe distance is ca. 1.9 Å (1.94(4) Å in  $[Fe^III Fe_3^II(OMe)_5(MeOH)_3(OBz)_4]$  [31] and 1.812(2) Å in a five-coordinate porphyrin [33]). Both the Fe<sup>II</sup>–O(H)Me [31] and Fe<sup>III</sup>–O(H)Me [34] distances are considerably longer, i.e. > 2.1 Å. The average M–OMe distance for the terminal ligands is 1.986(14) Å and 1.987(11) Å for **4** and **5** respectively. These observed distances are consistent with two terminal MeOH and two terminal  $[MeO]^-$  ligands on a disordered  $M_2^{III}M_2^{II}$  core. However, these data do not permit assignment of the metal atoms to the two oxidation states.

The Mössbauer spectral hyperfine parameters for **5** are given in Table 8 and the spectrum is shown in Fig. 4. These parameters are typical of high-spin Fe<sup>III</sup> and are far from those expected for high-spin Fe<sup>II</sup>. Although the Mössbauer spectral parameters do not rule it out, for coordination with oxygen ligands, low-spin Fe<sup>II</sup> is not likely [35]. The temperature dependence of the isomer shift and the spectral absorption area yield [36] an effective iron recoil mass of 75 g mol<sup>-1</sup> and a Mössbauer temperature of 180 K, values which are also indicative of the presence of high-spin iron(III) in the core. Therefore, the core of **5** is clearly Fe<sup>III</sup>Co<sup>II</sup>. Considering the similarities in the structures and other data for **4** and **5** it is likely that the former has an Mn<sup>III</sup>Co<sup>II</sup> core.

The Mössbauer spectral linewidth is sufficiently large that there must be more than a single iron environment. The spectrum can be fit with a constant isomer shift and a distribution of quadrupole splittings and is nearly equally well fit with two symmetric quadrupole doublets with an approximately 60 to 40% area ratio. The latter fit is consistent with the presence of the two isomers of **5** in an abundance that is statistical within experimental error. The resulting quadrupole splittings represent the extreme values expected for Fe<sup>III</sup> sites and are reasonable for this oxidation state in the clearly distorted coordination environment.

Magnetic susceptibility data for solid samples of **4** and **5** were collected in the temperature range 4.3–300.4 K. The data are displayed in Figs. 5 and 6. The complexes **4** and **5** are characterized by having high room temperature magnetic moments (**4**:  $\mu_{eff} = 9.78 \mu_B$  at 300.2 K; **5**:  $\mu_{eff} = 10.81 \mu_B$  at 300.4 K) which decrease upon cooling to  $\mu_{eff} = 3.51 \mu_B$  at 4.4 K (**4**) and  $\mu_{eff} = 2.98 \mu_B$  at 4.3 K (**5**). The measured effective magnetic moments at room temperature agree with the  $[M_2^{III}Co_2^{II}(OMe)_4]^{6+}$  formulation of the complex cores. The diamagnetic cobalt atoms in the cluster-ligand cause only a small contribution to the total magnetic susceptibility. The observed magnetic behavior is consistent with either weak antiferromagnetic coupling overall be-

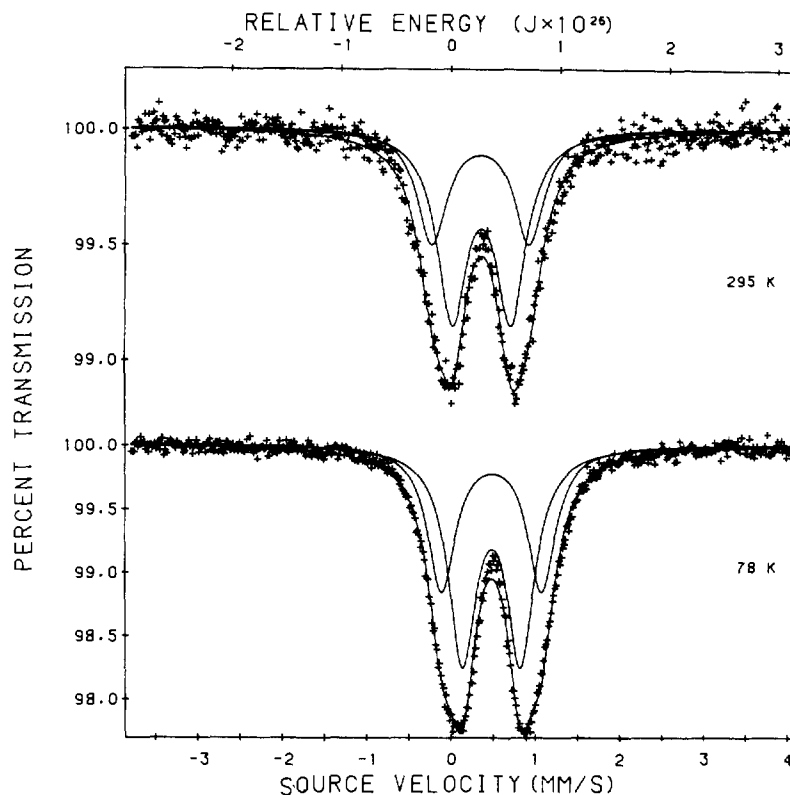


Fig. 4. The Mössbauer spectra of **5** showing a fit with two quadrupole doublets having the same shift but different quadrupole splittings.

tween the metal centers in the core and  $S = 0$  ground states, or with antiferromagnetic interaction between the molecules, or with zero-field splitting of the  $\text{Co}^{2+}$ -ions.

The magnetic characterization of the molecules is very complex because the  $\text{M}^{\text{III}}/\text{Co}^{\text{II}}$ -positions could not be crystallographically distinguished and because more than one coordination-isomer is present. If we try to explain the magnetic behavior in terms of only an intramolecular exchange interaction for the averaged molecule  $\text{M}_2^{\text{III}}\text{Co}_2^{\text{II}}(\text{OMe})_4$ , we can roughly estimate that the exchange parameter  $J_{ij}$  defined by  $H = -2\sum_{i,j} J_{ij} S_i S_j$ , does not exceed  $-10 \text{ cm}^{-1}$ .

As a result, the zero-field splitting of the  $\text{Co}^{\text{II}}$  ions is no longer a small perturbation but probably an equivalent or a dominant part of the overall interaction. Therefore, an interpretation of the magnetic properties based on an isotropic exchange Hamiltonian alone is not possible. Alternatively, by introducing the zero-field splitting parameters  $D$  and  $E$  into the equation, a fit of the experimental susceptibility data involves too many parameters.

The closely related tetranuclear compounds with cubane-like  $[\text{M}_4(\text{OMe})_4]^{4+}$ ,  $\text{M} = \text{Fe}, \text{Ni}$ , cluster-cores show ferromagnetic behavior [31,37]. Often, ferromag-

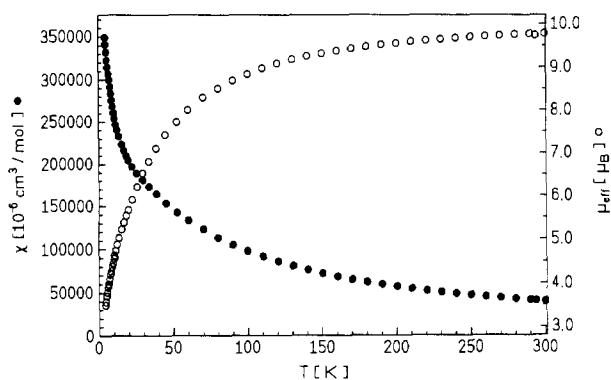


Fig. 5. Molar magnetic susceptibility data and effective magnetic moment vs. temperature for **4**. The solid lines result from the best fit to the theoretical expression given by van Vleck's equation.

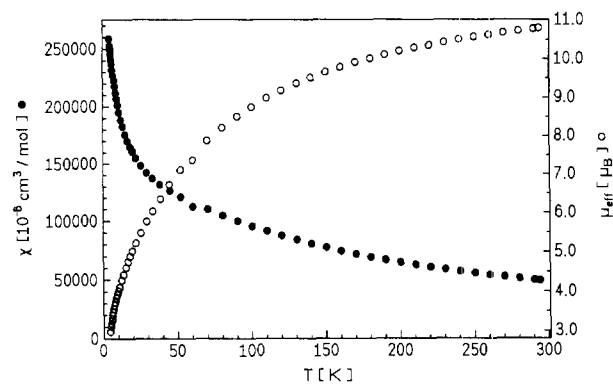


Fig. 6. Molar magnetic susceptibility data and effective magnetic moment vs. temperature for **5**. The solid lines result from the best fit to the theoretical expression given by van Vleck's equation.

netic as well as antiferromagnetic coupling takes place, e.g.  $M = \text{Mn, Ni, Cu}$  [32,38–40]. An antiferromagnetic interaction is dominant if the core is composed of different spin-centers [31,41], as is probably the case in this work as well. Note that, in addition to four  $\mu_3$ -methoxy-ligands, these new compounds have acetato-like bridging ligands which both provide another pathway for electronic exchange and cause additional distortions in the  $M_4(\text{OME})_4$  core.

### 3.3. Origin of the cluster cubes

It is known that the  $(\text{CO})_9\text{Co}_3\text{CR}$  cluster is not stable to oxidation [4]. In the case of  $\text{Hg}\{(\text{CO})_9\text{Co}_3\text{CCO}_2\}_2$  in THF, it appears that  $\text{Co}^{\text{II}}$  ion and  $\text{Hg}^0$  are generated by oxidation of some of the cluster ligands. As the  $\text{Co}^{\text{II}}$  ion is generated it is coordinated by intact cluster ligands at a rate such that crystalline **3** is precipitated. It is important to note that  $\text{Co}_4^{\text{II}}\text{O}\{(\text{CO})_9\text{Co}_3\text{CCO}_2\}_6$  is dissociated in THF (but not  $\text{CH}_2\text{Cl}_2$ ) and, as expected, **3** is readily converted into  $\text{Co}_4^{\text{II}}\text{O}\{(\text{CO})_9\text{Co}_3\text{CCO}_2\}_6$  when solid **3** is treated with  $\text{CH}_2\text{Cl}_2$ . This chemistry suggests that when redox reactions between the core metal ions and the cluster substituent are possible, coordination of the cluster ligand will be followed by subsequent, more complex, reactions. When **3** is treated with MeOH a complex reaction occurs and a compound having a double  $[\text{Co}_4(\text{OME})_4]$  cubane structure is isolated. Unfortunately, there are problems with the structure determination due to poor diffraction and the precise nature of this product remains unknown. However, these two observations suggest that the origins of **4** and **5** lie in similar reaction chemistry.

Slow cluster ligand dissociation from  $[\text{M}_2^{\text{II}}\{(\text{CO})_9\text{Co}_3\text{CCO}_2\}_4]$  in MeOH can lead to subsequent cobalt cluster degradation. The production of cobalt fragments including  $\text{Co}^{\text{II}}$  from cobalt carbonyl clusters is known [42]. Oxidation of the  $M^{\text{II}}$  centers, perhaps by  $[\text{Co}(\text{CO})_4]$  radicals, ultimately can yield the  $[\text{M}_2^{\text{III}}\text{Co}_2^{\text{II}}(\text{MeO})_6(\text{MeOH})_2\{(\text{CO})_9\text{Co}_3\text{CCO}_2\}_4]$  cluster cubes. The products isolated suggest that it is the  $M^{\text{II}}$  dimer that sequentially adds two solvated  $\text{Co}^{\text{II}}$  ions. There is only one way of adding the first but two different ways of adding the second  $\text{Co}^{\text{II}}$  unit, thereby generating the two isomeric forms of the cube.

The formation of the unusual carboxylate-bridged mixed-metal alkoxide cubes reported here can be attributed to (a) the electronic effects of the transition metal cluster on the basicity of the coordinating carboxylate functionality leading to rapid exchange with acetate, (b) the effect of the large carbonyl-covered surface of the cubes on its solubility, (c) the tendency of the tricobalt cluster to act as an in situ metered source of  $\text{Co}^{\text{II}}$  ions, and (d) the redox properties of the core metal ions promoted by a coordinating solvent, e.g. MeOH.

### Acknowledgements

The support of the National Science Foundation (XL, TF, CHE-9311885) and the Division of Materials Research of the National Science Foundation (GJL, DH, grants DMR-9214271, -9521739) is gratefully acknowledged. We thank Dr. Beisong Cheng and Professor W.R. Scheidt for aid in collecting the X-ray diffraction data for **4**.

### References

- [1] W. Cen, K.J. Haller, T.P. Fehlner, *Inorg. Chem.* 32 (1993) 995.
- [2] D. Seyferth, *Adv. Organomet. Chem.* 14 (1976) 97.
- [3] B.R. Penfold, B.H. Robinson, *Acc. Chem. Res.* 6 (1973) 73.
- [4] B.M. Peake, B.H. Robinson, J. Simpson, D.J. Watson, *Inorg. Chem.* 16 (1977) 405.
- [5] P.N. Lindsay, B.M. Peake, B.H. Robinson, J. Simpson, *Organometallics* 3 (1984) 413.
- [6] X. Meng, N.P. Rath, T.P. Fehlner, A.L. Rheingold, *Organometallics* 10 (1991) 1986.
- [7] R.C. Mehrotra, R. Bohra, *Metal Carboxylates*, Academic Press, New York, 1983.
- [8] W. Cen, K.W. Haller, T.P. Fehlner, *Inorg. Chem.* 30 (1991) 3120.
- [9] W. Cen, P. Lindenfeld, T.P. Fehlner, *J. Am. Chem. Soc.* 114 (1992) 5451.
- [10] S.W. Simerly, S.R. Wilson, J.R. Shapley, *Inorg. Chem.* 31 (1992) 5146.
- [11] S.R. Drake, B.F.O. Johnson, J. Lewis, G. Conole, M. McPartlin, *J. Chem. Soc. Dalton Trans.* (1990) 995.
- [12] T. Beringhelli, U. D'Alfonso, M. De Angelis, G. Ciani, A. Sironi, *J. Organomet. Chem.* 322 (1987) C21.
- [13] A. Ceriotti, R. Della Pergola, F. Demartin, L. Garlaschelli, M. Manassero, N. Masciocchi, *Organometallics* 11 (1992) 756.
- [14] R. Della Pergola, F. Demartin, L. Garlaschelli, M. Manassero, S. Martinengo, M. Sansoni, *Inorg. Chem.* 26 (1987) 3487.
- [15] T. Beringhelli, O. D'Alfonso, H. Molinari, A. Sironi, *J. Chem. Soc. Dalton Trans.* (1992) 689.
- [16] G. Hsu, S.R. Wilson, J.R. Shapley, *Inorg. Chem.* 30 (1991) 3882.
- [17] R.N. Grimes, *Adv. Inorg. Chem. Radiochem.* 26 (1983) 55.
- [18] R.N. Grimes, in: T.P. Fehlner (Ed.), *Inorganometallic Chemistry*, Plenum, New York, 1992, p. 253.
- [19] C.-S. Jun, D.R. Powell, K.J. Haller, T.P. Fehlner, *Inorg. Chem.* 32 (1993) 5071.
- [20] K.H. Whitmire, J. Ross, C.B. Cooper, D.F. Shriver, *Inorg. Synth.* 21 (1982) 66.
- [21] P. Chini, *J. Organomet. Chem.* 200 (1980) 31.
- [22] R.L. Sturgeon, M.M. Olmstead, N.E. Schore, *Organometallics* 10 (1991) 1649.
- [23] W. Cen, T.P. Fehlner, *Inorg. Synth.* 31 (1996) 228.
- [24] R.C.G. Killean, J.L. Lawrence, *Acta Crystallogr. Sect. B*: 25 (1969) 1750.
- [25] W.R. Scheidt, I. Turowska-Tyrk, *Inorg. Chem.* 33 (1994) 1314.
- [26] L. Merz, W. Haase, *J. Chem. Soc. Dalton Trans.* (1980) 875.
- [27] M.A. Baffares, L. Dauphin, X. Lei, W. Cen, M. Shang, E.E. Wolf, T.P. Fehlner, *Chem. Mater.* 7 (1995) 553.
- [28] J. Catterick, M.B. Hursthouse, P. Thornton, A.J. Welch, *J. Chem. Soc. Dalton Trans.* (1977) 223.
- [29] J.E. Davies, A.V. Rivera, G.M. Sheldrick, *Acta Crystallogr. Sect. B*: 33 (1977).

- [30] T.S. Gifeisman, A.A. Dvorkin, G.A. Tirnko, Y.A. Simonov, N.V. Gerbeleu, G.A. Popovich, *Izv. Akad. Nauk Mold. SSR. Ser. Fiz. Tekh. Mat. Nauk* 22 (1985) 2.
- [31] K.L. Taft, A. Caneschi, L.E. Pence, C.D. Delfs, G.C. Pappaefthymiou, S.J. Lippard, *J. Am. Chem. Soc.* 115 (1993) 11753.
- [32] M.A. Halcrow, J.-S. Sun, J.C. Huffman, G. Christou, *Inorg. Chem.* 34 (1995) 4167.
- [33] C. Lecomte, D.L. Chadwick, P. Coppens, E.D. Stevens, *Inorg. Chem.* 22 (1983) 2982.
- [34] K.L. Taft, D. Garfinkel-Shweky, A. Masschelein, S. Liu, A. Bino, S.J. Lippard, *Inorg. Chim. Acta* 198–200 (1992) 627.
- [35] W. Micklitz, V. McKee, R.L. Rardin, L.E. Pence, G.C. Pappaefthymiou, S.G. Bott, S.J. Lippard, *J. Am. Chem. Soc.* 116 (1994) 8061.
- [36] R.D. Ernst, D.R. Wilson, R.H. Herber, *J. Am. Chem. Soc.* 106 (1984) 1646.
- [37] J.E. Andrews, A.B. Blake, *J. Chem. Soc. A:* (1969) 1456.
- [38] W.L. Gladfelter, M.W. Lynch, D.N. Hendrickson, H.B. Gray, *Inorg. Chem.* 20 (1981) 2390.
- [39] E.A. Schmitt, L. Noodleman, E.J. Baerends, D.N. Hendrickson, *J. Am. Chem. Soc.* 114 (1992) 6109.
- [40] L.E. Pence, A. Caneschi, S.J. Lippard, *Inorg. Chem.* 35 (1996) 3069.
- [41] J.A. Bertrand, T.C. Hightower, *Inorg. Chem.* 12 (1973) 206.
- [42] G. Albanesi, E. Gavezzotti, *Lincei Rend. Sc. Fis. Mat. Nat.*, 41 (1966) 497.